Dynamics of the phase transition of the fully polymerized and deuterated diacetylene 2,4-hexadiynylene bis(*p*-toluenesulfonate)

J. Even, M. Bertault, B. Toudic, and H. Cailleau
Groupe Matière Condensée et Matériaux, Université de Rennes 1, Campus Beaulieu, 35042 Rennes Cedex, France

J. L. Fave
Groupe de Physique des Solides, Universités de Paris 6 et 7, 2 Place Jussieu, 75251 Paris Cedex 05, France

R. Currat
Institut Laue-Langevin, Boîte Postale 156X, 38042 Grenoble Cedex, France

F. Moussa
Laboratoire Léon Brillouin (CEA-CNRS), CE Saclay, 91191 Gif-sur-Yvette Cedex, France
(Received 7 April 1993; revised manuscript received 13 September 1993)

Coherent neutron scattering and Raman scattering with IR sources were used to make a dynamical study of the structural transition of the disubstituted and fully deuterated diacetylene 2,4-hexadiynylene bis(*p*-toluenesulfonate) (pTS-D) in the monocrystalline polymer state. This compound may undergo a progressive polymerization in the crystalline state, which gives a quasiunique opportunity to obtain large size monocrystals of conjugated polymer. A second-order-like transition takes place at $\sim T_c = 182$ K; it is associated to motions of the polar side groups. We achieved a dynamical study of a soft mode which is clearly observed in the high-temperature phase (neutron) as in the low-temperature phase (Raman) and is characterized by overdamping on approaching T_c. In addition the growth of a central peak is observed above T_c. We show that this structural instability presents an intermediate character between order disorder and displacive, with a more pronounced displacive character than in the monomer crystal.

I. INTRODUCTION

Diacetylenes (R-C≡C-C≡C-R′) are compounds which can present a unique chemical property: Some of them undergo a topochemically controlled solid state polymerization in crystalline state.[1] The best known and the most investigated compound of this family is the symmetrical diacetylene 2,4-hexadiynylene bis(*p*-toluenesulfonate) where $R = R' = CH_3\text{-}C_6H_4\text{-}SO_2\text{-}O\text{-}CH_2$ and referred to as pTS-H hereafter. The main motivation for the interest in pTS is that large crystals of monomer transform into polymer single crystal of nearly perfect crystalline quality by exposure to radiation (X, UV, γ) or by thermal annealing (Fig. 1). When obtained from this last procedure, pTS-H polymer is produced homogeneously in the monomer matrix; in other words the mixed monomer-polymer system forms a series of solid solutions which covers the entire composition range from $X = 0$ to $X = 1$ in polymer content. The polymer chains extend along a crystallographic axis (**b** axis in the monoclinic structure of pTS).

Another interesting property of pTS-H is that structural phase transitions occur both in the monomer and polymer crystals, but structural instabilities have been observed also in mixed monomer-polymer crystals with high- and low-polymer content. The structure of both high- and low-temperature phases of monomer and polymer were determined to be monoclinic (space group $P2_1/c$).[2-4] The transitions are associated with librational motions of the highly polar side groups, yielding a doubling of the unit cell along the **a** crystallographic axis and two inequivalent site for each structural unit. In addition an intermediate modulated phase along the **b** axis was discovered by Robin *et al.*[5] in the monomer crystal; it exists in monomer-polymer mixed crystals of pTS-H up to at least 10% of polymer content.[6]

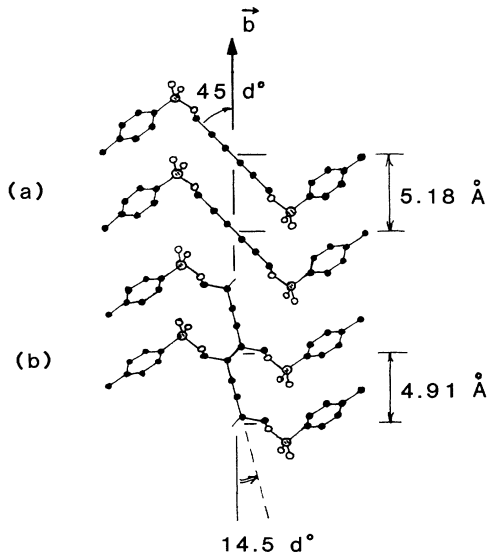

FIG. 1. Projection of the crystal structures of pTS-H on the (**b**,**c**) plane: (a) monomer and (b) polymer (Ref. 44).

The structural instabilities have been studied by x-ray and neutron diffraction,[6-8] by differential scanning calorimetry[9] (DSC), and by dielectric measurements.[10] The static properties of the incommensurately modulated phase have been particularly well investigated in the monomer. Not so much information is available on the single phase transition which takes place at T_c in the polymer crystal. This transition appeared continuous in most experimental studies.[11-13] Terauchi, Ueda, and Hatta[14] found a first-order-like transition by x-ray diffraction. Bloor *et al.*[15] analyzed results from different spectroscopic techniques: resonant Raman scattering, reflection spectroscopy, and far-infrared absorption spectroscopy. These authors deduced the value of the critical exponent and they pointed out that it is close to the value obtained from a two-dimensional Ising model.

It is already known that the structural instabilities in pTS-H are connected to torsional motions of the *p*-toluene sulfonate side groups. However, as the side group carries a permanent dipole along the phenyl ring axis, we made a better determination of the displacements associated to the order parameter: This analysis shows that the phase transition is associated with important changes in dipole-dipole interactions as indicated in a direct study of the dielectric properties of pTS-H single crystals.[10] We achieved a comparison of high- and low-temperature structures of pTS-D polymer performed with x rays[16] as it was made for pTS-H polymer.[4] In this latter work comparison of the two structures involves only a rotation of the side groups around the C_4-C_7 axis of the phenyl ring (axis corresponding to the $\mathbf{e}_2$ vector in the Table I). In fact, comparison of both structures in pTS-D polymer (our x-ray study) shows that the CD_3 and SO_2 groups move in opposite directions when two different structural units are forming on the two inequivalent sites in the low-temperature unit cell. An analysis of thermal motions by the rigid-body method[17,18] taking the phenyl ring as the rigid group confirms this observation: It shows that the main librational motion occurs around the $\mathbf{v}_{11}$ vector for the side groups (Table I, Fig. 2). This motion exists in the high-temperature phase; it is probably the precursor for the transition which leads to the two different positions occupied by the side groups on the two low-temperature inequivalent sites.

The dynamics associated with the structural instability was not understood. It was not possible to resolve by x-ray studies whether or not the precise description of thermal motions of molecules was in agreement with an order-disorder or a displacive character for this transition.[15] It should be also pointed out Bloor *et al.* stated that a soft mode had been observed by far-infrared spectroscopy.[15] However a soft mode cannot be observed in a pTS-H polymer crystal with this experimental technique because the crystallographic space group is centrosymmetric. This observation showed nevertheless that modes are coupled to the order parameter and undergo a progressive broadening on approaching the transition temperature.

TABLE I. Benzene group librational tensor L at $T=293$ K. Eigenvalues $\mathbf{L}_{ii}$ and components of the eigenvectors $\mathbf{v}_{ii}$ on the $\mathbf{e}_i$ vectors.

	v_{11}	v_{22}	v_{33}
*e*1	−0.491	0.267	−0.829
*e*2	0.871	0.117	−0.477
*e*3	0.031	−0.957	−0.290
L_{ii} (deg^2)	117	16	6

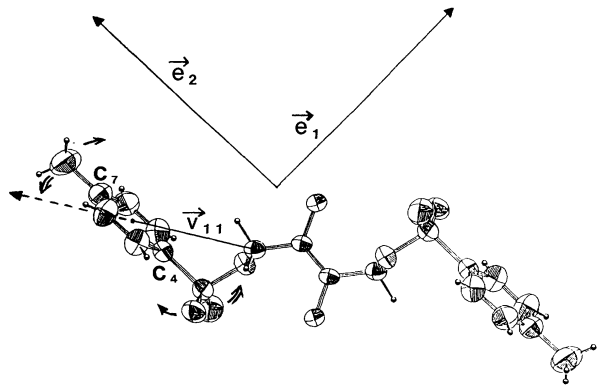

FIG. 2. The pTS-D molecule as viewed in a $(\mathbf{e}_1,\mathbf{e}_2)$ plane; $\mathbf{e}_1$ vector is perpendicular to the benzene ring, $\mathbf{e}_2$ vector is parallel to the C_4-C_7 direction. $\mathbf{v}_{11}$ represents the principal axis of the side-group rotation.

Direct studies of the dynamics of this phase transition were undertaken by neutron and Raman scattering: Preliminary results have been presented in Ref. 19. In this work, experimental methods are described in Sec. II. The calorimetric results are described in Sec. III. In Sec. IV we present the results obtained from neutron scattering in the high-temperature phase. Section V concerns the Raman-scattering study in the low-temperature phase. Section VI brings together all the results obtained in this study and attempts to present a coherent description of the structural instability which takes place at T_c in the fully deuterated pTS polymer crystal.

II. EXPERIMENTAL DETAILS

A. Crystal growth and polymerization

It was necessary to synthesize and to grow large size single crystals of fully deuterated pTS-D in order to perform elastic and inelastic coherent neutron-scattering experiments. We have synthesized and purified pTS-D according to a long and complex series of procedures described elsewhere.[20] Single crystals of monomer were obtained from solutions of the purified material by a controlled evaporation of the solvent (acetone) with nitrogen gas at 277 K. Then these monocrystals were polymerized during 30 h by thermal annealing at 333 K. The curves of isothermal polymerization kinetics obtained at 333 K in a DSC7 calorimeter with pTS-D monocrystals show indeed that about 24 h are necessary to bring the reaction to completion and to obtain pTS-D polymer crystals.[20]

B. Calorimetric measurements

A preliminary calorimetric experiment was performed on Perkin-Elmer DSC7 differential scanning calorimeter controlled by a PC-AT for data acquisition and processing. In the range between 125 and 225 K, the measurement head of the apparatus was cooled with liquid nitrogen and flushed with dry helium gas. The temperature calibration was made using the phase transition (186.1 K) and the melting point (279.7 K) of cyclohexane;[21] energy was calibrated using the enthalpy of the phase transition of cyclohexane (79.58 $J\,g^{-1}$). The accuracy of the isobarically measured specific heat was checked against a plate of sapphire standard (130.03 mg) from 140 to 225 K. pTS-D polymer (weighing 51 and 54 mg) and pTS polymer (68 mg) monocrystal samples were encapsulated in 50 μl aluminum pans in order to ensure a good heat transfer; the same heating rate of 10 K/min was used for calibration and measurements.

C. Neutron scattering

We used a crystal of 0.5 cm^3 for neutron scattering. The neutron measurements were carried out on the three-axis spectrometer IN14 using a cold-neutron source at Institut Laue-Langevin in Grenoble with pyrolitic graphite monochromator and analyzer. The incident neutron wave vector was first held fixed at 2.662 $Å^{-1}$ (14.7 meV) and a graphite filter was used to remove high-order neutrons from the beam. The width (full width at half maximum) in energy of the resolution function in this configuration was 220 GHz for vanadium. In a second configuration we used a 5-meV incident neutron energy ($ki = 1.55$ $Å^{-1}$) and a beryllium filter cooled with liquid nitrogen; the width in energy of the resolution function was 40 GHz for vanadium. The scattering plane was chosen ($\mathbf{a}^*, \mathbf{b}^*$) because **b** is the direction of polymerization and also the direction of incommensurability in the monomer crystals and **a** is the cell-doubling axis in the low-temperature phase. Constant-Q scans were performed in order to record inelastic neutron-scattering spectra. The crystal was cooled using an helium cryostat down to 10 K.

D. Raman scattering

The high absorption of pTS polymer crystals in the visible[11,22] requires use of IR lasers for Raman scattering. The first one was a dye laser tuned to $\lambda = 8540$ Å (styryl 9M) but the best results were obtained at a longer wavelength (10 923 Å) with an ionized argon laser used with mirrors for the infrared region. In both cases the incident light power was $P = 20$ mW. The resolution of the spectrometer (Jobin-Yvon Ramanor U1000) was on the order of 1 cm^{-1} and a germanium detector cooled with liquid nitrogen was used. A few spectra were recorded at room temperature with a YAG laser ($\lambda = 10\,642$ Å with $P = 10$ mW). The emission bands were observed only with (**b**,**b**) polarization (A_g symmetry) parallel to the polymer chains. The same crystal (0.25 cm^3) of pTS-D polymer was used for all the Raman-scattering studies.

III. CALORIMETRIC RESULTS

Figure 3 shows the specific heat as a function of temperature in the range (140 K, 225 K) of two different pTS-D polymer monocrystals. The first curve (a) refers to a crystal obtained from the same synthesis as the monocrystals used in this work for neutron and Raman scattering; curve (b) refers to a single crystal obtained from a more recent synthesis corresponding to modified and improved preparation procedures. This second synthesis has probably provided a material of certainly better purity[16,20] and of high quality in deuteration which has been controlled by deuterium NMR indicating around 99% D on toluene radical and 95% D on CD_2 radical. For comparison, curve (c) refers to a pTS-H polymer crystal.

These two pTS-D samples present a qualitatively similar behavior: an endotherm with a somewhat rapid increase and a smoother decay which spreads over about 40 K; but the two anomalies of Cp present a shift in temperature of about 10°. The transition temperatures, calculated by considering the endotherms as characteristic of second-order transitions,[23] correspond to the half value of the maximum of the specific-heat jumps and are about 188 K for (a) (Fig. 4) and 196 K for (b); on the other hand the temperature corresponding to the maximum of the specific-heat jump (Fig. 4) is ~180 K for (a). We note also that the shape of the anomaly of Cp somewhat

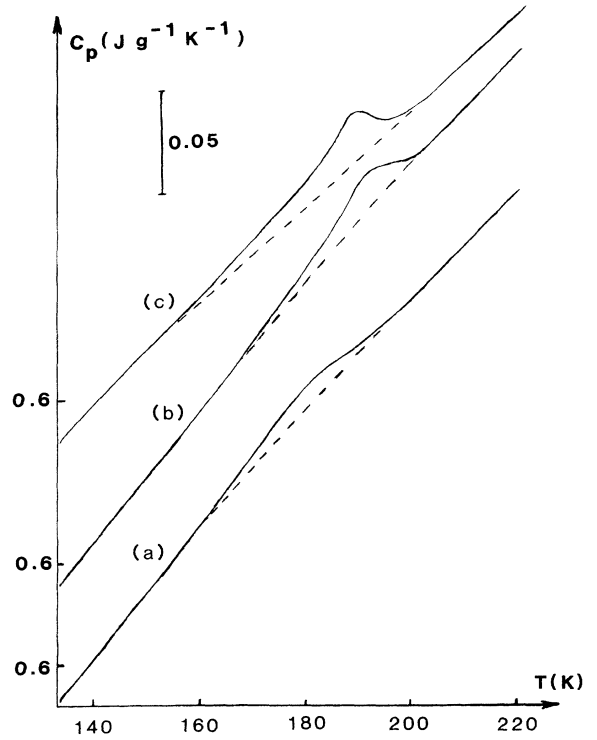

FIG. 3. Heat capacity as a function of temperature, measured on pTS-D and pTS polymer monocrystals: (a) pTS-D polymer crystal issued as the ones used for neutron and Raman scattering, from the same synthesis; (b) pTS-D polymer crystal issued from a different synthesis; (c) hydrogenated pTS polymer crystal.

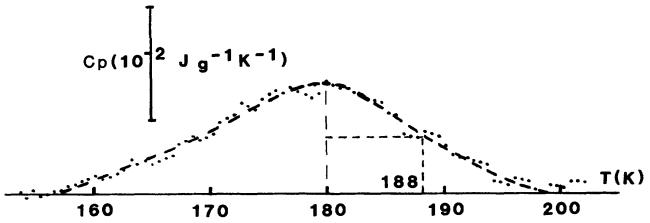

FIG. 4. Excess heat capacity observed for the pTS-D monocrystal referred as (a) in Fig. 3.

differs depending on the synthesis of the material. Whereas there is a clear signature for the single crystal (b) obtained from more recent synthesis material, this signature is more rounded for the crystal (a) obtained from the same synthesis as all the crystals used in this work. This actually shows the important role that impurities may play on the phase transition.

The quantitative analysis of our data is then given here only for the polymer crystal (a), since this is the crystal used in Raman and neutron scattering. The excess of Cp shown for (a) in Fig. 4 is obtained after substraction between the experimental Cp curve and a fitted line which describes the "normal" nontransitional heat capacity between approximately 160 and 200 K [dotted line in Fig. 3(a)]. The maximum of the specific-heat jump is clearly smaller (2.5 times in this case) than the one observed on the Cp curve of hydrogenated pTS polymer crystal (c) shown in Fig. 3. The values of the enthalpy and the entropy of the transition are, respectively, 91 $J\,mol^{-1}$ and 0.51 $J\,mol^{-1}\,K^{-1}$. The values are smaller than the ones found for polymer crystal (b) (respectively, 128 $J\,mol^{-1}$ and 0.68 $J\,mol^{-1}\,K^{-1}$) and for pTS-H polymer crystal (c) (respectively 188 $J\,mol^{-1}$ and 1.03 $J\,mol^{-1}\,K^{-1}$), which presents a transition temperature at about 196 K.

IV. NEUTRON SCATTERING

A. Elastic study

As stated before, the high-temperature space group is $P2_1/c$ and there is a doubling of unit cell along the **a** axis below the transition temperature T_c. The low-temperature space group is $P2_1/n$ using the same crystallographic axes (**2a**,**b**,**c**) or $P2_1/c$ using (**a'**,**b'**,**c'**) with $\mathbf{a}'=-\mathbf{c},\mathbf{b}'=\mathbf{b},\mathbf{c}'=2\mathbf{a}+\mathbf{c}$. The systematic extinctions for $P2_1/c$ are $(h,0,l)$ $l=2n$ and $(0,k,0)$ $k=2n$.

The strongest superstructure reflection reached in the (**a***,**b***) plane was (6.5,1,0) using an incident neutron wave-vector value of $ki=2.662$ Å^{-1}. Figure 5 shows the variation of the integrated intensity for the (6.5,1,0) superlattice reflection as a function of temperature. The evolution of the intensity appears continuous, which is consistent with a second-order or weakly first-order phase transition. Above T_c, strong diffuse scattering is observed, indicating the existence of pretransitional critical fluctuations associated to short-range order. They correspond to the existence of low-frequency excitations which are integrated with the given energy resolution (220 GHz).

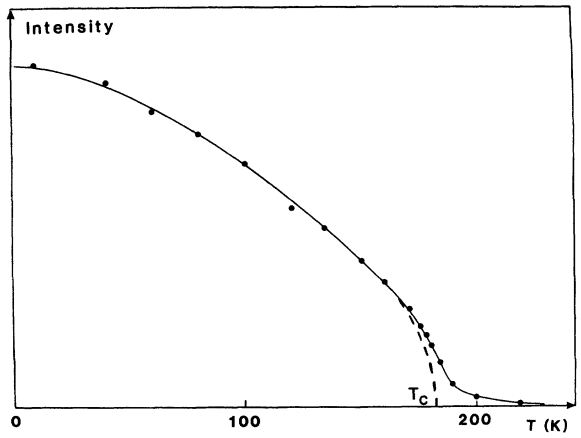

FIG. 5. Integrated intensity of the (6.5,1,0) superlattice reflection as a function of temperature ($ki=2.662$ Å^{-1}). The broken line going T_c ($T_c=182$ K is determined after drawing from Fig. 6) is a guide for eyes to show the existence of critical scattering near T_c, assuming its value at $T\leq T_c$ is twice as small as the same value measured at $T\geq T_c$.

The transition temperature $T_c=182\pm2$ K was determined after drawing (Fig. 6) the variation of the full widths at half maximum of the (6.5,1,0) superstructure reflection corresponding to the critical scattering along **a*** and **b*** as a function of temperature. Δq_a and Δq_b measured in the low-temperature phase are the widths of Bragg peaks which are limited by the resolution. The transition temperature T_c was found to be equal to 182 K in extrapolating the width variation of the critical scattering peaks. The ratio ξ_b/ξ_a of the correlation lengths along the two axes **a*** and **b*** is equal to 1.7 at $T=200$ K. In this case, ξ_a and ξ_b were obtained by folding of Gaussian with Lorentzian including the background. The study indicates weak anisotropy in the (**a***,**b***) plane although it was not really performed as a function of temperature.

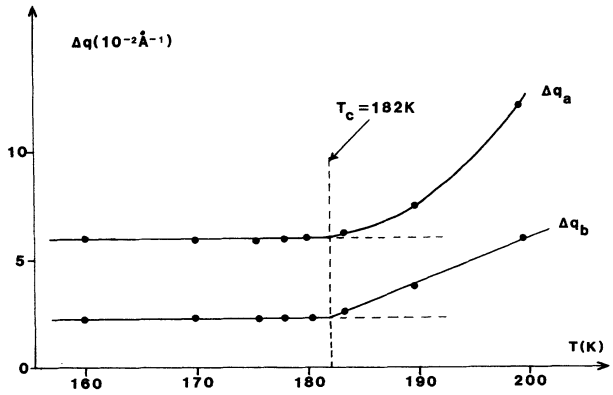

FIG. 6. Evolution of the full widths at half maximum of the (6.5,1,0) superlattice reflection along **a***(Δq_a) and **b***(Δq_b) directions as a function of temperature ($ki=2.662$ Å^{-1}). Δq_a and Δq_b were obtained directly from the experimental results without fitting.

The value of the critical exponent was estimated at $\beta=0.25\pm0.05$ from the variation of integrated intensity of the (6.5,1,0) reflection as a function of temperature for $T_c=182$ K. The variation of this intensity is scaled as a function of (T_c-T) on a log-log plot (Fig. 7). In this diagram, the intensity follows the power law $I=I_0(T_c-T)^{2\beta}$ on a large temperature range going from $T=8$ K to about $T=170$ K. Taking into account the fact that critical scattering supplies around T_c an additional contribution to the intensity, and assuming the value of this contribution at $T\leq T_c$ is twice as small as the value measured at $T\geq T_c$, the corrected intensity follows the power law with $\beta=0.25$ from $T=8$ K to T_c. A D-NMR study of the resonance lines of the same pTS-D polymer crystal versus temperature leads to a value for β in good agreement with this one.[24] Finally we point out that above T_c the diffuse scattering is really centered on the (0.5,0,0) zone-boundary point and not on incommensurate positions as in the monomer crystal.

B. Dynamical study

Inelastic neutron-scattering spectra were recorded at the (2.5,1,0) point of the reciprocal lattice with an improved resolution in energy (40 GHz at $ki=1.55$ Å^{-1}) in the (200–280 K) temperature range. A low-frequency mode is detected at $T=280$ K (Fig. 8); its frequency decreases and its damping increases with decreasing temperature. This soft mode becomes overdamped around $T=240$ K. In addition, the elastic peak (Fig. 8) grows on approaching T_c. At $T=280$ K the incoherent elastic-scattering contribution represents in intensity an amount of 70% of the elastic peak; in addition it is weakly temperature dependent. Figure 9 gives the evolution of the central peak integrated intensity, which increases when $T\rightarrow T_c$.

We have also performed energy scans at different distances (expressed in reduced units) from the zone-boundary point (2.5,1,0) in the **a*** and the **b*** directions at $T=280$ K and $T=218$ K. Figure 10 depicts the evolution of the neutron-scattering inelastic spectrum along **b*** at $T=218$ K. The lowest part represents the contribution of the soft mode which is overdamped in the (a) position and clearly underdamped in the (d) position. The second contribution corresponds to the elastic incoherent scattering which is assumed to be almost constant in the q range. The upper contribution has an energy width almost equal to the energy width of the resolution. This central peak has also a q-space extension along **a*** and **b***. The central peak and the elastic incoherent scattering peak were fitted to Gaussian functions which had the energy width of the resolution function and were centered at $\omega=0$.

In a first stage a set of quasiharmonic frequencies and damping constants were obtained for the soft mode directly from a damped harmonic oscillator function:

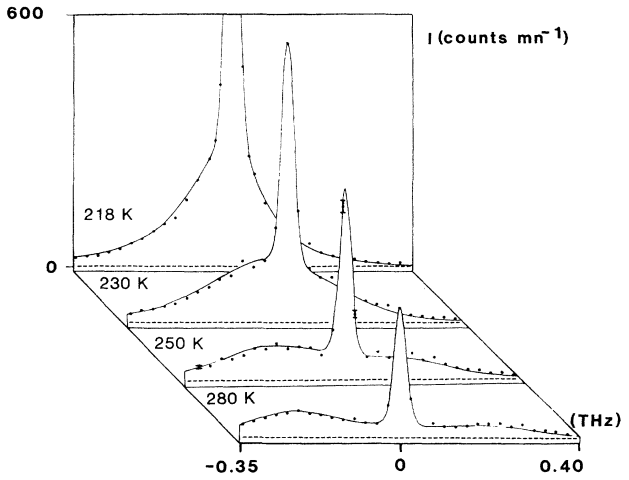

FIG. 8. Inelastic neutron-scattering spectra of pTS-D polymer in the high-temperature phase and measured at the (2.5,1,0) point of reciprocal space ($ki=1.54$ Å^{-1}). A soft mode and a central peak are observed, the elastic incoherent peak being measured away from the (2.5,1,0) critical point of the reciprocal lattice and substracted in the fits.

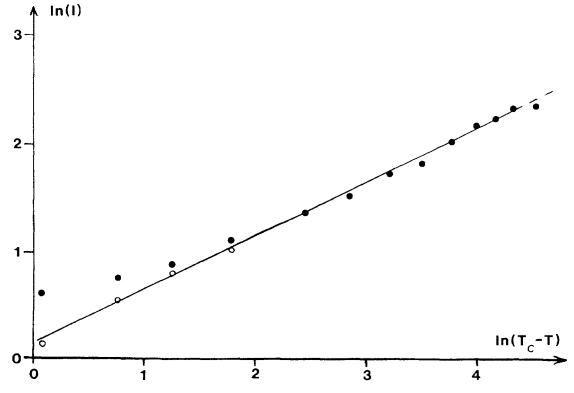

FIG. 7. A log-log plot of integrated intensity of (6.5,1,0) superlattice reflexion as a function of temperature. Full circles correspond to experimental data; the four open circles correspond to the corrected values of intensity. The straight line is in agreement with a β value equal to 0.25.

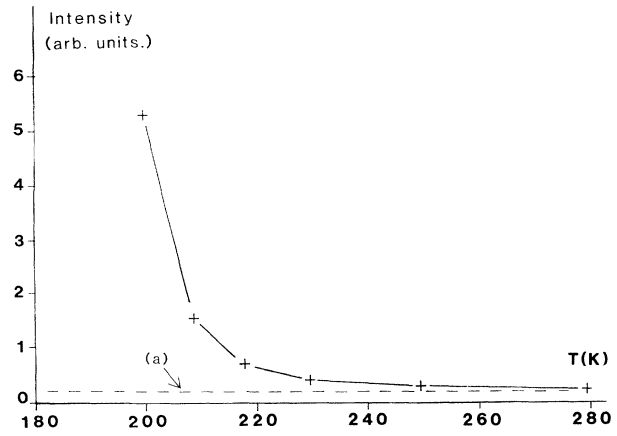

FIG. 9. Evolution of the central peak intensity, as a function of temperature, at the (2.5,1,0) point and for $ki=1.54$ Å^{-1}; (a) contribution of elastic incoherent scattering.

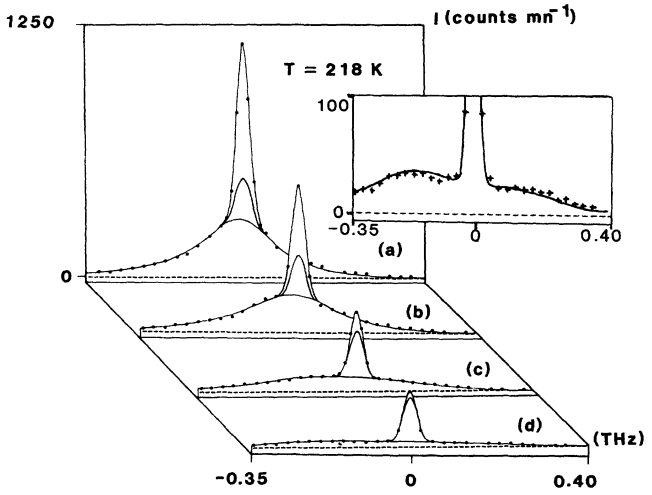

FIG. 10. Evolution of the inelastic neutron-scattering spectra at $T=218$ K along the $\mathbf{b}^*$ direction: (a) at $\mathbf{q}_c=(2.5,1,0)$, (b) at $\mathbf{q}_c-0.025\mathbf{b}^*$, (c) at $\mathbf{q}_c-0.050\mathbf{b}^*$, (d) at $\mathbf{q}_c-0.075\mathbf{b}^*$. The lowest curve represents the contribution of the soft mode, the intermediate curve the contribution of the elastic incoherent scattering and the upper curve the contribution of the central peak. In the inset, enlargement of the inelastic-scattering spectrum (d) shows the underdamped soft mode.

$$S(\mathbf{Q},\omega)\sim\frac{\omega\Gamma_q|F(\mathbf{Q})|^2}{(1-e^{-\hbar\omega/k_BT})[(\omega^2-\omega_q^2)^2+\omega^2\Gamma_q^2]}\ .$$

This function was convoluted with the instrumental resolution function. In the overdamped regime at $T\leq 218$ K and close to the critical wave vector, the scattering cross section of the soft mode may be reduced to

$$S(q,\omega)\sim\frac{1/\tau_q}{\omega^2+(1/\tau_q)^2}$$

with $1/\tau_q=\omega_q^2/\Gamma_q$. This signature is equivalent to the order-disorder one, where $1/\tau_q$ is the critical relaxation rate. One should however keep in mind that the displacive character of the transition is clearly established going away from q_c: in Fig. 10, a frequency ω_q becomes visible at $q=q_c-0.075\mathbf{b}^*$.

Critical relaxation rates were then extracted and fitted to a dispersion law,

$$1/\tau_q=\omega_q^2/\Gamma_q=1/\tau_{q=q_c}+D_aq_a^2+D_bq_b^2\ ,$$

where q_a,q_b are defined by the relation

$$\mathbf{q}=\mathbf{q}_c+q_a\mathbf{a}^*/a^*+q_b\mathbf{b}^*/b^*,$$

$$\mathbf{q}_c=2.5\mathbf{a}^*+\mathbf{b}^*,\quad D_a=6.9\ \text{THz Å}^2,\quad D_b=16.5\ \text{THz Å}^2\ .$$

The ratio ξ_b/ξ_a is equal to the square root of D_b/D_a,[25] we find $\xi_b/\xi_a=1.5$; this value is in good agreement with the result obtained in the static study (Sec. IV A).

The half widths at half maximum of the central peak integrated intensity distribution along $\mathbf{a}^*$ and $\mathbf{b}^*$ (L_a^{-1} and L_b^{-1}) were determined at $T=218$ K. The ratio L_b/L_a was found to be equal to 1.9, showing that the anisotropies of the central peak and soft mode in q space are similar.

In this neutron-scattering study we wish to describe the dynamics on approaching T_c [T_c,T_c+50 K] by relaxation processes ($1/\tau_c\simeq 400[(T-T_c)/T_c]$ GHz). It is interesting to note that the relaxation rate in typical order-disorder cases, such as p-terphenyl, $1/\tau_c=32[(T-T_c)/T_c]$ GHz ($T_c=179.5$ K).[26] The value for pTS-D polymer is closer to the one found in anthracene-TCNB, $1/\tau_c=591[(T-T_c)/T_c]$ GHz ($T_c=197$ K), this compound presenting also a displacive phase transition with some order-disorder character.[27]

In a second stage we have analyzed our data obtained for the central peak and the soft mode above T_c with a phenomenological model used previously for structural phase transitions in crystals with perovskite structure ($SrTiO_2$, $KMnF_3$, . . .).[28] The frequency spectrum of the fluctuations in the soft-phonon branch corresponds to the following dynamical susceptibility:

$$\chi^{-1}=\omega_c^2-\omega^2-i\omega\Gamma_c-i\omega\frac{\delta^2}{\gamma-i\omega}\ ,$$

where ω_c vanishes at T_c. Assuming that $\Gamma_c\ll\delta^2/\gamma$, $\omega_\infty^2=\omega_c^2+\delta^2\gg\gamma$, $k_BT\gg\hbar\omega$, one has

$$S(q,\omega)\sim\frac{k_BT}{\pi}\left[\frac{\Gamma_c}{(\omega_\infty^2-\omega^2)^2+\omega^2\Gamma_c^2}+\frac{\delta^2}{\omega_\infty^2\omega_c^2}\frac{\gamma'}{\omega^2+\gamma'^2}\right]$$

with $\gamma'=\gamma\omega_c^2/\omega_\infty^2$.

The first part of the expression describes the response function for the soft mode; its frequency ω_∞ remains finite at T_c: $\omega_\infty(T_c)=\delta$. The second part corresponds to the central peak: After integration over ω, its intensity varies according to $k_BT\delta^2/\omega_c^2\omega_\infty^2$. As the soft mode is overdamped up to at least 230 K, the frequencies ω_∞ were deduced from the integration of its intensity k_BT/ω_∞^2. The parameter δ was calculated and plotted as a function of temperature (Fig. 11). The renormalized

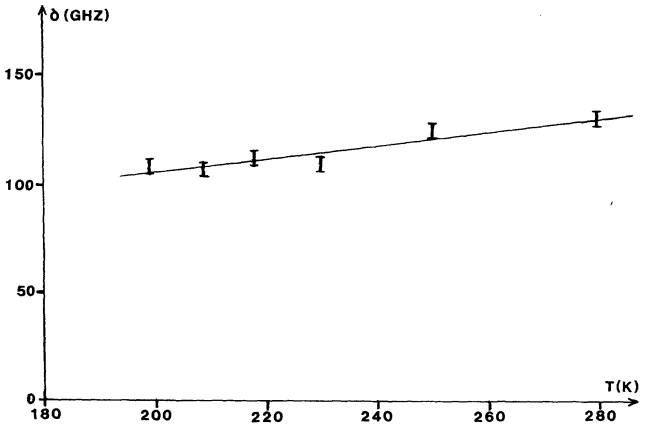

FIG. 11. Evolution of the parameter δ (phenomenological model) as a function of temperature. The error bars refer to the statistical uncertainty in determination of the integrated intensities.

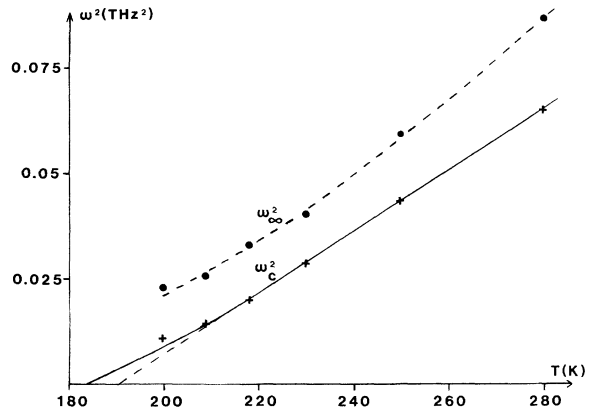

FIG. 12. Temperature dependence of ω_c^2 and ω_∞^2 (phenomenological model). Calculations were made using the integrated intensities of the central peak and soft mode for pTS-D polymer.

frequency ω_c of the soft mode has a mean-field behavior up to at least T_c+30 K, in accordance with the following expression:

$$\omega_c^2 = a(T - T_0)$$

with $T_0 = 190$ K and $a = 7.3\times10^{-4}$ THz^2 K^{-1} (Fig. 12).

V. RAMAN SCATTERING

A. Low-frequency modes

The low-frequency modes were observed in (**b**,**b**) polarization (A_g symmetry). We made symmetry assignment of the soft mode at high and low temperature. There are indeed only four one-dimensional irreducible representations at the A point of the Brillouin zone [zone boundary at $\mathbf{q}=(0.5,0,0)$] and at the Γ point (zone center).

A	E	C_2	I	σ_h
A_g	+1	+1	+1	+1
B_g	+1	−1	+1	−1
A_u	+1	+1	−1	−1
B_u	+1	−1	−1	+1

Γ	E	C_2	I	σ_h
A_g	+1	+1	+1	+1
B_g	+1	−1	+1	−1
A_u	+1	+1	−1	−1
B_u	+1	−1	−1	+1

The compatibility relations between the A point above T_c and the Γ point below T_c are

$$A \leftrightarrow \Gamma ,$$

$$A_g \leftrightarrow B_g ,$$

$$B_g \leftrightarrow A_g ,$$

$$A_u \leftrightarrow B_u ,$$

$$B_u \leftrightarrow A_u .$$

Thus the soft mode can be observed below T_c only in A_g symmetry by Raman scattering. Dimensionality of the order parameter is equal to one. The experimental bands were fitted to a damped harmonic oscillator function as previously indicated (Sec. IV A).

A first study was performed over the (13–270 K) temperature range with excitation line at $\lambda=8540$ Å (Fig. 13). The frequency of the band corresponding to the soft mode is located around 27 cm^{-1} at 13 K; it decreases while the damping increases on approaching T_c: The soft mode cannot be observed at high temperature.

There is another interesting band with a frequency equal to 37 cm^{-1} at 13 K. This frequency decreases up to T_c and becomes almost constant above T_c. A more careful study was carried out with the excitation line of the ionized argon laser at $\lambda=10\,923$ Å in the (130–210 K) temperature range (Fig. 14). It allowed to make a better evaluation of the band's width variation. Figure 15 shows the results obtained for the band with frequency equal to 37 cm^{-1} at 13 K. The frequency variation as a function of temperature shows clearly that the corresponding mode is coupled to the order parameter. But the most interesting feature is the behavior of the damping of this mode around T_c. The "inflexion point" on the $\Gamma(T)$ curve corresponds to the transition temperature. Such a behavior is encountered for example in the study of the order-disorder transition of the *p*-terphenyl molecular crystal at atmospheric pressure;[29] it is also the behavior of the same crystal and of *p*-quaterphenyl under high pressure[30,31] when the transitions become more

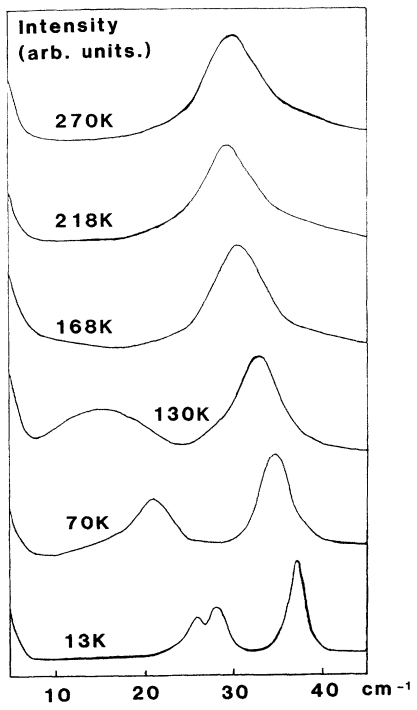

FIG. 13. Low-frequency Raman spectra for pTS-D polymer in (**b**,**b**) polarizations, recorded at $\lambda=8540$ Å. The lowest-frequency mode, which is broadening on approaching T_c and disappearing at T_c, is the soft mode.

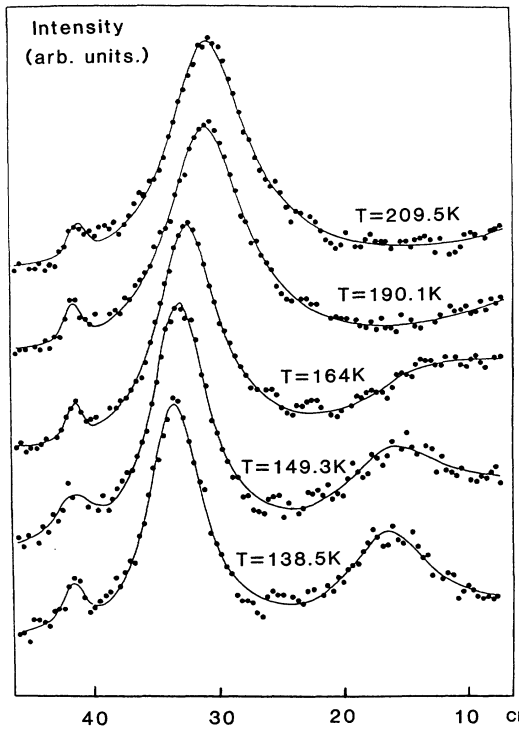

FIG. 14. Low-frequency Raman spectra for pTS-D polymer in (**b**,**b**) polarizations, recorded at $\lambda = 10\,923$ Å. Note the presence of another mode in addition to the soft mode, whose width and frequency vary versus temperature.

displacive but remain with some order-disorder character. The linewidth broadening in the low-temperature phase may be related to the progressive setting of disorder when the temperature increases. Indeed, when disorder exists, the crystal is spatially inhomogeneous. This induces a dispersion of vibrational frequencies which gives rise to a mode broadening. The inflexion point observed on the $\Gamma(T)$ curve may result from the additional contribution which is due to disorder and is important around the transition. Indeed, far from the transition, the linewidth is only determined by anharmonicity in the low- and high-temperature phases.

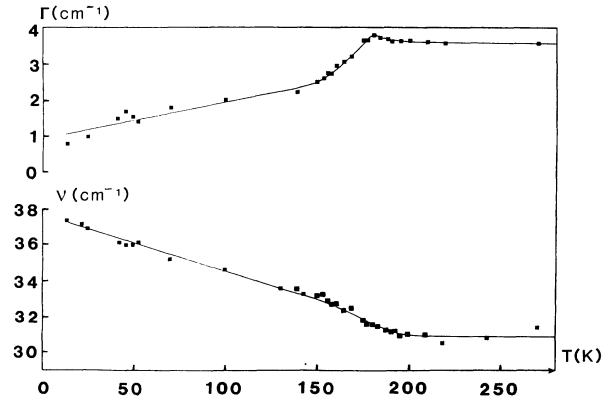

FIG. 15. Behavior of the width Γ and frequency ν of the mode observed at $\nu = 37$ cm^{-1} at $T = 13$ K, as a function of temperature in pTS-D polymer. The continuous lines are guide for the eyes.

B. High-frequency modes

Four predominant high-frequency vibrational modes in the (500 cm^{-1}, 2500 cm^{-1}) range were detected at room temperature in pTS polymer crystals by resonant Raman scattering: 952, 1203, 1485, 2086 cm^{-1}.[32] In this study, four bands were observed in pTS-D polymer crystals: 774, 1258, 1466, 2080 cm^{-1} (Fig. 16). They correspond mainly to the high-frequency vibrational modes of an isolated polydiacetylene. They are treated for pTS polymer in a model[33] of a collection of point masses where only nearest-neighbor harmonic forces are used to describe stretching and bending internal coordinates in the plane containing the diacetylene rod. This model shows in particular that the fourth mode is not related to any displacement of the fully hydrogenated or deuterated side groups. No change indeed is observed for the frequency of this mode when going from pTS polymer to pTS-D polymer.

The most interesting feature is that the phase transition has an effect on high-frequency vibrational modes. Indeed the first two modes in pTS polymer (952, 1203) undergo a splitting below T_c, which becomes maximum at very low temperature. According to the previous simulation, the splitting is related to the existence of two inequivalent polymer chains per unit cell at $T \leq T_c$. Splitting observation of the 1485 cm^{-1} line in pTS polymer is prevented by a coupling of this mode with the scissors motion at the frequency of 1464 cm^{-1} of the CH_2 group at the joint of the diacetylene rod and the benzene sulfonate radicals. This coupling does not exist in pTS-D polymer because the difference between both frequencies is much higher, and the splitting of the 1466 cm^{-1} is observed in pTS-D polymer at $T \leq T_c$ (Fig. 17). The spectra were fitted with three peaks at $T \leq T_c$ and two peaks at $T \geq T_c$. The best-fit frequencies are plotted in Fig. 18: One can see that the three modes are coupled to the order parameter; T_c can then be estimated to ~ 182 K as indicated with the dashed line in the figure. One of the two modes ν_1 or ν_2 is active at the zone boundary at high temperature (B_g symmetry) and becomes active at the

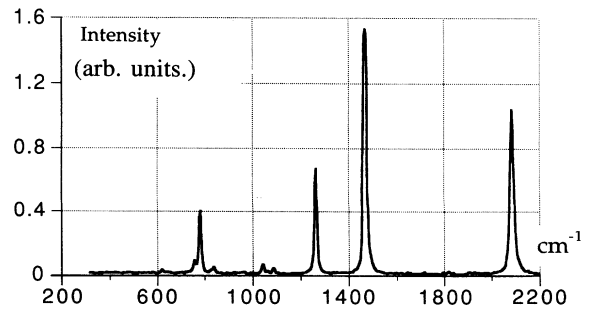

FIG. 16. High-frequency Raman spectrum of pTS-D polymer recorded at room temperature with exciting line $\lambda = 10\,642$ Å.

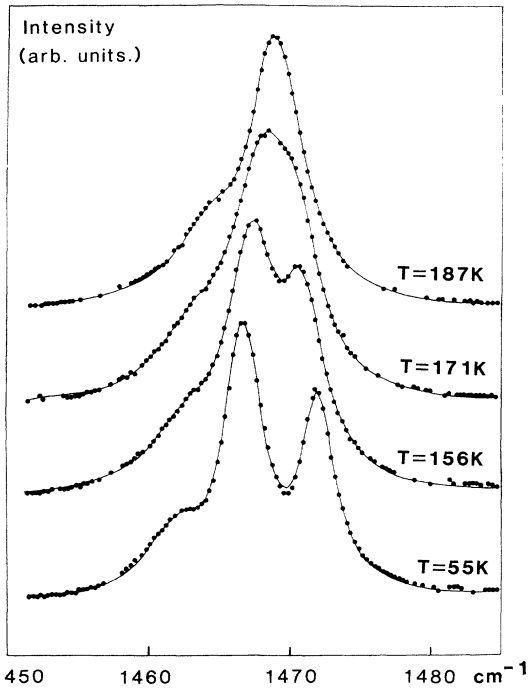

FIG. 17. Evolution of Raman spectra of pTS-D polymer as a function of temperature, recorded in the frequency range (1450–1485 cm^{-1}) with exciting line $\lambda = 10\,923$ Å.

zone center at $T \leq T_c$ (A_g symmetry). The expression of the first coupling term in the Landau expansion as a function of the normal coordinate Q of this mode and of the order parameter η is then $\eta^2 Q^2$. This frequency ν_1 is then affected in accordance with the equality $\nu_1^2 = A_1 \pm B_1 \eta_{eq}^2$. The other mode is active at the zone center (A_g symmetry) below and above T_c; then the expression of the first coupling term is $\eta^2 Q$ and it leads to the same type of variation for the ν_2 frequency: $\nu_2^2 = A_2 \mp B_2 \eta_{eq}^2$. It is a reasonable assumption to say that the two lines ν_1 and ν_2 belong to the same phonon branch at $T \geq T_c$, as the compatibility relation between the Γ point and the A point is

$$A \leftrightarrow \Gamma ,$$

$$A_g, B_g \leftrightarrow A_g, B_g ,$$

$$A_u, B_u \leftrightarrow A_u, B_u .$$

Bloor *et al.*[15] assumed that the splitting $\Delta\nu$ between ν_1 and ν_2 varies according to a power law

$$\Delta\nu \propto (T_c - T)^{\beta} .$$

(β is the critical exponent associated to the order parameter.)

To establish such a relation for the splitting $\Delta\nu$, the coefficient A_1 must be made equal to the coefficient A_2. In other words, one supposed that this phonon branch has no dispersion along the **a*** direction. Indeed the coupling between the polymer chains is weak, particularly for the internal modes of the polymer backbone; making this further assumption, we find the following analytical relation:

$$\Delta\nu \propto (T_c - T)^{2\beta} .$$

In Fig. 19, full circles (1) correspond to the experimental value $\Delta\nu = \nu_1 - \nu_2$ with $\Delta A = A_1 - A_2 = 0$. A value $\beta = 0.22$ for the critical exponent is deduced from the drawn straight line. This value is slightly smaller than 0.25 given by neutron study (Sec. IV A). It is possible to obtain a better agreement between both methods if for example $\Delta A' = \Delta A / 2\nu_m$ is taken equal to 0.3 cm^{-1} ($\Delta A'$ represents the resultant splitting at $T = T_c$); this corresponds to open circles (2) in Fig. 19 and to a critical exponent value equal to 0.25 when deduced from the drawn straight line. It is not possible to indicate the case which may correspond to the real experimental situation. Indeed the arbitrary value $\Delta A' = 0.3$ cm^{-1} is much smaller than the resolution of the spectrometer (on the order of 1 cm^{-1}); this $\Delta A'$ induces however a significant

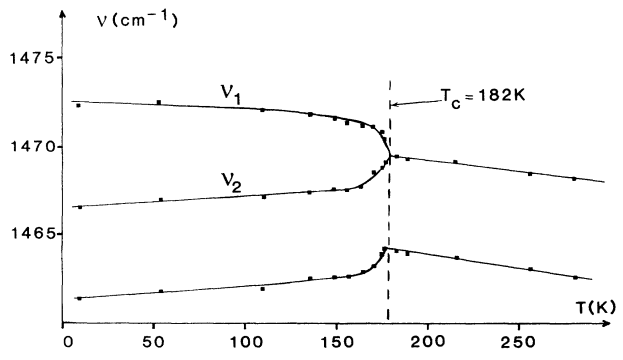

FIG. 18. Evolution of the mode frequencies (showed in Fig. 15) as a function of temperature. The lines are the result of a fit with two modes in the high-temperature phase and with three modes in the low-temperature phase.

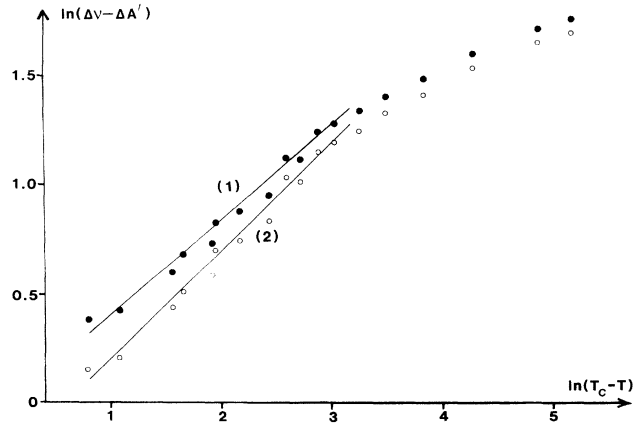

FIG. 19. A log-log plot of $(\Delta\nu - \Delta A')$ as a function of $(T_c - T)$. $\Delta\nu = \nu_1 - \nu_2$: ν_1 and ν_2 are the frequencies showed in Fig. 16 (for $\Delta A'$, see text). Full circles (1) correspond to $\Delta A' = 0$ and a critical exponent $\beta = 0.22$; open circles (2) correspond to $\Delta A' = 0.3$ cm^{-1} and a 0.25 value for β.

variation of the β value. That shows Raman scattering is not a suitable method to make an accurate study of the critical exponent; the presence of a third mode (see Figs. 17 and 18) also makes the fitting procedure more difficult. The expression $\Delta\nu \propto (T_c - T)^{2\beta}$ shows then that the previous interpretation of Bloor *et al.* based on their spectroscopic measurements has to be reconsidered. Finally we point out that the range of the quadratic coupling seems to extend from T_c to about $T = 160$ K (Fig. 19).

VI. DISCUSSION

Calorimetric measurements lead to consider the transition to have a second-order-like signature. Neutron- and Raman-scattering studies indicate also that the transition appears continuous. Calorimetric results have shown also that the entropy of the transition for the polymer pTS-D crystals studied in this work (0.51 $J\,mol^{-1}\,K^{-1}$) is intermediate between the one found for the biphenyl [0.13 $J\,mol^{-1}\,K^{-1}$ (Ref. 34)] where the transition has a displacive character,[35] and the value given by R ln2 (5.8 $J\,mol^{-1}\,K^{-1}$) for an ideal order-disorder transition. Indeed ideal situations seldom happen with molecular crystals, distinction between displacive and order disorder being difficult. That is, for example, the case for anthracene-TCNB,[36,37] bis(4-chlorophenyl)sulfone,[38] hydrogenated and deuterated *p*-terphenyl.[39] In our case, the intermediate character between order disorder and displacive for the transition in the polymer pTS-D is based on the results obtained by Raman and neutron scattering.

Using elastic and inelastic coherent cold-neutron and Raman scatterings, we have succeeded in obtaining a complete description of the dynamics in the polymer crystal of pTS-D. The transition appears continuous and the pretransitional dynamics are associated with the softening of a phonon branch; the soft mode presents a heavy damping (Fig. 20) on approaching the transition temperature T_c. By combination of the results of both neutron and Raman scattering, we are able to represent the pretransitional dynamics of pTS-D polymer in the whole temperature range 13–293 K (Fig. 20). On approaching T_c when coming from low or high temperature, the soft-mode frequency is clearly decreasing. However, in both cases the mode is overdamped near T_c, preventing the study of frequency as a function of temperature. It is a fact that near T_c the soft mode has been analyzed in the neutron study using the scattering cross section for relaxation processes.

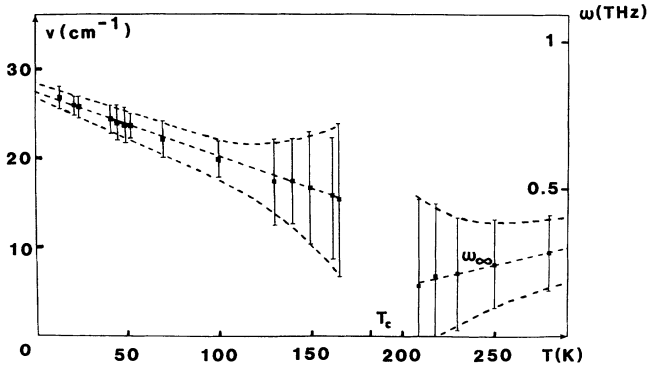

FIG. 20. Temperature dependence of the soft-mode frequency and damping Γ (full height of the bars) for pTS-D polymer in the high-temperature phase (neutron scattering) and in the low-temperature phase (Raman scattering). The dashed lines are guides for eyes showing the decreasing of the soft-mode frequency and increasing of damping Γ on approaching T_c.

The dynamics of pTS-D monomer and polymer are remarkably close. It is only slightly more displacive in the polymer state with a soft mode which becomes overdamped between T_c and at least $T_c + 80$ K in the monomer and $T_c + 50$ K in the polymer.[40] This behavior can be connected to the contraction along the stack *b* axis during solid-state polymerization, which hinders the motions of the side groups.

We have also shown that the previous order-parameter analysis based on spectroscopic measurements was wrong. A two-dimensional character of the phase transition, involving the ($\mathbf{a}^*$,$\mathbf{c}^*$) plane,[15] does not provide a good description of the phase transition in pTS-D polymer because the correlation lengths along $\mathbf{a}^*$ and $\mathbf{b}^*$ are not very different. The strong dependence with temperature of the superlattice intensity near T_c may suggest the occurrence of a weakly first-order phase transition associated to a negative fourth-order term in the Landau expansion (the third-order term is forbidden by symmetry).

In our opinion the behavior of the central peak in pTS-D polymer (Sec. IV B) may be related to the presence of defects in the crystal, as incomplete polymerization, residual hydrogen atoms or impurities (see Sec. III, Calorimetric measurements). Indeed it has been shown that the polymer chains include about 100–200 monomer units in the polymer crystal.[41] The phenomenological model described in Sec. IV B can be connected to a model involving the influence of defects as it was shown by Halperin and Varma for $SrTiO_3$.[42]

The control of the synthesis and of the polymerization procedure permits us to obtain mixed crystals with any polymer content X, so as to be able to study different samples with a well defined X in all the range between 0 to 1.[20] Experimental results we have already obtained by microcalorimetric,[16] dielectric,[10] and Raman-neutron-scattering[43] methods seem to indicate that, in a mixed monomer-polymer crystal, no long-range order occurs related to the structural instability in the range $0.15 \leq X \leq 0.55$ although the average lattice remains fairly crystalline. Thus, the system presents some analogies with orientational glasses as in mixed-crystals solids, but, in our case, with another type of static disorder. The understanding of dynamics of the structural instabilities in both pure monomer and polymer pTS-D crystals is important for interpretation of the more complex situation encountered in the mixed crystals.

ACKNOWLEDGMENTS

We thank L. Toupet for the x-ray data acquisition. The Groupe Matière Condensée et Matériaux is "Unité Associée au CNRS No. 804." The Groupe de Physique des Solides is "Unité Associée au CNRS No. 17."

[1]G. Wegner, Z. Naturforsch. **24b**, 824 (1969).
[2]J. P. Aime, J. Lefebvre, M. Bertault, M. Schott, and J. O. Williams, J. Phys. (Paris) **43**, 307 (1982).
[3]Von Kobelt and E. F. Paulus, Acta Crystallogr. B **30**, 232 (1974).
[4]V. Enkelmann, Acta Crystallogr. B **33**, 2842 (1977).
[5]P. Robin, J. P. Pouget, R. Comes, and A. Moradpour, J. Phys. (Paris) **41**, 415 (1980).
[6]J. N. Patillon, P. Robin, P. A. Albouy, J. P. Pouget, and R. Comes, Mol. Cryst. Liq. Cryst. **76**, 297 (1981).
[7]J. P. Aime, Ph.D. thesis, University Paris VII, 1983.
[8]H. Grimm, D. Axe, and C. Krohnke, Phys. Rev. B **25**, 1709 (1982).
[9]M. Bertault, A. Collet, and M. Schott, J. Phys. (Paris) Lett. **42**, L-131 (1981).
[10]R. Nowak, J. Sworakowski, B. Kuchta, M. Bertault, M. Schott, R. Jakubas, and H. A. Kolodziej, Chem. Phys. **104**, 467 (1986).
[11]D. Bloor, F. H. Preston, and D. J. Ando, Chem. Phys. Lett. **38**, 33 (1976).
[12]D. N. Batchelder and D. Bloor, Chem. Phys. Lett. **38**, 37 (1976).
[13]W. Rehwald, A. Vonlanthen, and W. Meyer, Phys. Status Solidi **75**, 219 (1983).
[14]H. Terauchi, T. Ueda, and I. Hatta, J. Phys. Soc. Jpn. **50**, 3472 (1981).
[15]D. Bloor, D. A. Fisher, D. N. Batchelder, R. Kennedy, A. C. Cottle, W. F. Lewis, and M. B. Hursthouse, Mol. Cryst. Liq. Cryst. **52**, 83 (1979).
[16]J. Even, Ph.D. thesis, University Paris VI, 1992.
[17]D. W. J. Cruickshank, Acta Crystallogr. **9**, 754 (1956).
[18]V. Schomaker and K. N. Trueblood, Acta Crystallogr. B **24**, 63 (1968).
[19]J. Even, M. Bertault, B. Toudic, H. Cailleau, J. L. Fave, M. Schott, F. Moussa, and R. Currat, Ferroelectrics **125**, 51 (1992).
[20]M. Bertault, Ph.D. thesis, University Paris VII, 1983.
[21]J. G. Aston, G. J. Szaz, and H. L. Fink, J. Am. Chem. Soc. **65**, 1135 (1943).
[22]B. Reimer, H. Baessler, J. Hesse, and G. Weiser, Phys. Status Solidi **73**, 709 (1976).
[23]I. Hatta, T. Nakayama, and T. Matsuda, Phys. Status Solidi A **62**, 243 (1980).
[24]J. Etrillard, Ph.D. thesis, University Rennes I, 1993.
[25]B. Dorner and R. Comes, in *Dynamics of Solids and Liquids by Neutron Scattering,* edited by S. W. Lovesey and T. Springer, Topics in Current Physics No. 3 (Springer-Verlag, Berlin, 1977).
[26]H. Cailleau, Ph.D. thesis, University Rennes I, 1981.
[27]P. Bourges, Ph.D. thesis, University Rennes I, 1989.
[28]S. M. Shapiro, J. D. Axe, G. Shirane, and T. Riste, Phys. Rev. B **6**, 4332 (1972).
[29]A. Girard, H. Cailleau, Y. Marqueton, and C. Ecolivet, Chem. Phys. Lett. **54**, 479 (1978).
[30]A. Girard, Y. Delugeard, and H. Cailleau, J. Phys. (Paris) **48**, 1751 (1987).
[31]A. Girard, Y. Delugeard, L. Pichon, and L. Toudic, J. Phys. I (France) **2**, 1833 (1992).
[32]D. N. Batchelder and D. Bloor, J. Phys. C **11**, 3005 (1982).
[33]W. F. Lewis and D. N. Batchelder, Chem. Phys. Lett. **60**, 232 (1979).
[34]T. Atake and H. Chihara, Solid State Commun. **35**, 131 (1980).
[35]A. Bree and M. Edelson, Chem. Phys. Lett. **46**, 500 (1977).
[36]C. Ecolivet, M. Bertault, A. Mierzejewski, and A. Collet, in *Dynamics of Molecular Crystals,* edited by J. Lascombe (Elsevier, New York, 1987), p. 187.
[37]P. Bourges, M. H. Lemee-Cailleau, P. Launois, F. Moussa, H. Cailleau, C. Ecolivet, and A. Mierzejewski, Ferroelectrics **109**, 69 (1990).
[38]J. Etrillard, B. Toudic, M. Bertault, J. Even, M. Gourdji, A. Peneau, and L. Guibe, J. Phys. (Paris) **3**, 2437 (1993).
[39]H. Cailleau and D. Dworkin, Mol. Cryst. Liq. Cryst. **50**, 217 (1979).
[40]J. Even, H. Cailleau, B. Toudic, M. Bertault, F. Moussa, and R. Currat, Physica B **180**, 339 (1992).
[41]M. Orczyk, J. Sworakowski, and M. Bertault, Progr. Colloid Polymer Sci. **80**, 21 (1989).
[42]B. I. Halperin and C. M. Varma, Phys. Rev. B **14**, 4030 (1976).
[43]S. Longeville, M. Bertault, J. Even, J. L. Fave, and F. Moussa (unpublished).
[44]V. Enkelmann and G. Wegner, Angew. Chem. **16**, 416 (1977).